

ADAPTIVE HOMOGENEITY-DIRECTED DEMOSAICING ALGORITHM

Keigo Hirakawa and Thomas W. Parks

Electrical and Computer Engineering
Cornell University
Ithaca, NY 14853

kh237@cornell.edu, parks@ece.cornell.edu

ABSTRACT

Most cost-effective digital camera uses a single image sensor, applying alternating patterns of red, green, and blue color filters to each pixel location. Demosaicing algorithm reconstructs a full three-color representation of color images from this sensor data. This paper identifies three inherent problems often associated with directional interpolation approach to demosaicing algorithms: misguidance color artifacts, interpolation color artifacts, and aliasing. The level of misguidance color artifacts present in two images can be compared using metric neighborhood modeling. The proposed demosaicing algorithm estimates missing pixels by interpolating in the direction with fewer color artifacts. The aliasing problem is addressed by applying filterbank techniques to directional interpolation. The interpolation artifacts are reduced using a nonlinear iterative procedure. Experimental results using digital images confirm the effectiveness of this approach.

1. INTRODUCTION

In a typical digital camera, the optical image formed at the image plane is captured by a single CCD or CMOS sensor array, which samples the image according to a color filter array (CFA). Fig. 1 shows the popular Bayer pattern [1]. A demosaicing algorithm is a method for reconstructing a full three-color representation of color images by estimating the missing pixel components. Simple plane-wise interpolation frequently results in color artifacts because the proportions of red, green, and blue are corrupted at object boundaries. Because the like colors never appear adjacent to each other in Bayer pattern, the output image often suffers from a pattern of alternating colors, referred to as *zippering* (Fig. 2).

Introducing structure between different color channels helps overcome these difficulties. Algorithms [2][3] hypothesize that the quotient of two color channels is slowly varying, following the fact that two colors occupying the same coordinate in the chromaticity plane have equal ratios between the color components. Alternatively, [4][5][6][7] assert that the differences between red, green, and blue images are slowly varying.

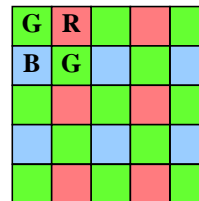


Fig. 1. Bayer Color Filter Array Pattern

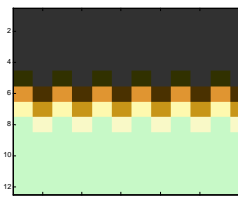


Fig. 2. Zippering Artifact

This principle is motivated by the observation that the color channels are highly correlated. The difference image between green and red (blue) channels contains low-frequency components only. A more sophisticated color channel correlation model is explored in [9]. Moreover, [3][6][8] incorporate edge-directionality. Interpolation along an object boundary is preferable to interpolation across this boundary for most images.

The above algorithms produce good results in general. The demosaicing algorithm proposed in this paper differs from other existing algorithms because it models the color artifact using homogeneity. By addressing the color artifact problem explicitly, the algorithm demonstrates a significant improvement in the output image quality.

2. METRIC NEIGHBORHOOD MODEL REVIEW

Metric neighborhood modeling offers a systematic method to identify a group of pixels that are similar. Let X be a set of two-dimensional pixel positions, and Y be a set of CIERGB tri-stimulus values [11][12]. Then a color image $f: X \rightarrow Y$ is a mapping between pixel locations and tri-stimulus values.

The neighborhood map $M_f: X \times \mathfrak{R} \rightarrow 2^X$ will be defined as a function from X and \mathfrak{R} to the set of all subsets of X . An important example of neighborhood maps is the domain ball neighborhood B . Let $d_X(\cdot, \cdot)$ be

a distance function in X and $\delta \in \mathfrak{R}$. Define $B(x, \delta)$ as a set of points in X that are within δ distance from $x \in X$

$$B(x, \delta) = \{p \in X \mid d_x(x, p) \leq \delta\}. \quad (1)$$

Similarly, neighborhood maps can be established using the range of f . With *a priori* knowledge that the end user is a human, pixels are discriminated using a distance metric in CIELAB space (represented by the set \hat{Y}) [10]. The color space conversion map is denoted as $\pi: Y \rightarrow \hat{Y}$, $\pi([R, G, B]^T) = [L, a, b]^T$. Let d_L be a Euclidean distance function of the luminance component, and d_C be a Euclidean distance function in the a - b plane. Define a level neighborhood L_f and a color neighborhood C_f as:

$$\begin{aligned} L_f(x, \varepsilon_L) &= \{p \in X \mid d_L(f(x), f(p)) \leq \varepsilon_L\} \\ C_f(x, \varepsilon_C) &= \{p \in X \mid d_C(f(x), f(p)) \leq \varepsilon_C\}. \end{aligned} \quad (2)$$

Define a metric neighborhood U_f as

$$U_f(x, \delta, \varepsilon_L, \varepsilon_C) = B(x, \delta) \cap L_f(x, \varepsilon_L) \cap C_f(x, \varepsilon_C). \quad (3)$$

If $x_0 \in U_f(x, \delta, \varepsilon_L, \varepsilon_C)$ then we expect that $f(x)$ appears similar to $f(x_0)$. Let $|\cdot|: 2^X \rightarrow \mathfrak{R}$ be the size of the set. Homogeneity is a tool designed to analyze the behavior of U_f . Define a homogeneity map $H_f: X \times \mathfrak{R}^3 \rightarrow \mathfrak{R}$ as

$$H_f(x, \delta, \varepsilon_L, \varepsilon_C) = |U_f(x, \delta, \varepsilon_L, \varepsilon_C)| / |B(x, \delta)|. \quad (4)$$

3. HOMOGENEITY-DIRECTED DEMOSAICING ALGORITHM

Section 3.1 describes a method to compare the levels of color artifacts present in two images using homogeneity map (4). The direction to interpolate is chosen to minimize the level of color artifacts. Due to the rectangular sampling lattice in Bayer pattern, interpolation is performed in horizontal and vertical directions only (see Fig. 1). Directional interpolation uses filterbank techniques to cancel aliasing from CFA sampling (section 3.2). Section 3.3 shows ways to suppress color artifacts.

3.1. Homogeneity and Artifacts

Demosaicing algorithms with a directionality selection approach suffer from two types of color artifacts. The first type is called *misguidance* color artifact. The misguidance occurs when the direction of interpolation is *erroneously* selected. The second type of color artifact is associated with limitations in the interpolation. That is, even with a *perfect* directional selector, the interpolation

algorithm may not reconstruct the color image perfectly. In this paper, this phenomenon is referred to as *interpolation* artifact. Normally interpolation artifacts are far less objectionable than misguidance artifacts, although they are still noticeable. A method to reduce interpolation artifacts is discussed in section 3.3.

A homogeneity map (4) can be used to compare the levels of misguidance color artifacts present in two images. We hypothesize that the misguidance color artifacts occur as *isolated* events. When an image is interpolated in the direction orthogonal to the orientation of the object boundary, the color that appears at the pixel of interest is unrelated to the physical object represented. Fig. 2 illustrates this point clearly. Thus a pixel marked by severe color artifacts has few pixels nearby that are similar, and its homogeneity map value is small.

Demosaicing algorithms with a directionality selection approach suffer from discontinuities in the output images due to frequent switching from interpolation in one direction to another. Taking a spatial average of the homogeneity map eliminates the discontinuity problem.

3.2. Interpolation

In this section, horizontal interpolation technique is presented (vertical interpolation done similarly). Let $R(\cdot)$, $G(\cdot)$, and $B(\cdot)$ represent red, green, and blue color plane images, respectively, and $n \in X$. Assume $G(n) - R(n)$ is slowly varying [4][5][6][7]. That is, the high frequency components of the difference images decay more rapidly than that of $G(n)$.

First, a method to reconstruct $G(\cdot)$ from sampled green and red pixels is developed. In the green-red row of Bayer pattern (Fig. 3), the even samples of green image and the odd samples of red image are given. Given $G(n)$, let $G_0(n)$ and $G_1(n)$ denote even and odd sampled-signals of $G(n)$. That is,

$$G_0(n) = \begin{cases} G(n) & n \text{ even} \\ 0 & n \text{ odd} \end{cases} \quad G_1(n) = \begin{cases} 0 & n \text{ even} \\ G(n) & n \text{ odd} \end{cases}. \quad (5)$$

Note $G(n) = G_0(n) + G_1(n)$ (Lazy wavelet [13]). G_0 is available directly from the Bayer pattern, but G_1 is not (Fig. 3). To investigate how to obtain G_1 , consider filtering G with a linear filter h : $y(n) = h(n) * G(n)$. We would like h to have the property that $y(n) = G_1(n)$: an example of $h(n)$ is an ideal low pass filter, when G is band-limited. Let h_0 and h_1 be the even and odd sampled-signals of h ; let R_1 be the odd sampled-signal of R . Then

$$G(n) = G_0(n) + h_1(n) * G_0(n) + h_0(n) * G_1(n). \quad (6)$$

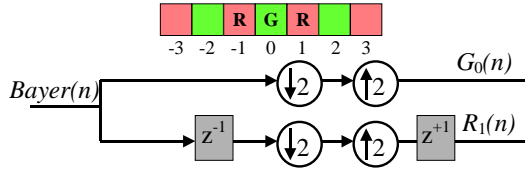


Fig. 3. Green-Red Row of Bayer Array.

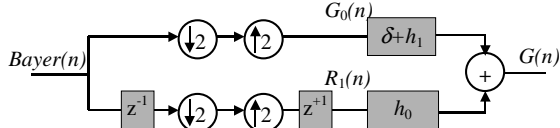


Fig. 4. Proposed method to estimating $G(n)$ (8).

Even-sampled signal $h_0(n)$ is chosen such that the sampled-difference signal $G_1(n) - R_1(n)$ is attenuated:

$$h_0(n) * G_1(n) \approx h_0(n) * R_1(n). \quad (7)$$

Substituting (7) into (6),

$$G(n) = G_0(n) + h_1(n) * G_0(n) + h_0(n) * R_1(n). \quad (8)$$

Equation (8) is a method to estimate G from G_0 and R_1 only (same technique used for G_0 and B_1). See Fig. 4. Because of the filterbank structure, alias cancellation is implicit in (8). Readers are encouraged to verify that alias terms in G_0 channel are cancelled by the terms in the R_1 .

To design an FIR filter $h(n)$ which meets (7) and $y(n) = G(n)$, solve the following optimization problem:

$$\hat{h}_{opt}(\xi) = \arg \min_h \left\| \hat{w}(\xi) (1 - \hat{h}(\xi)) \right\|^2 \quad (9)$$

where $\hat{\cdot}$ denotes the Fourier transform, $h(n)$ is length 5, weighting function is $\hat{w}(\xi) = 2\pi - |\xi|$, and $\hat{h}_0(\xi = 0) = \hat{h}_0(\xi = \pi) = 0$ to ensure (7). Using minimization tools in Matlab, we find

$$h_{opt}(n) = [-0.2569, 0.4339, 0.5138, 0.4339, -0.2569] \approx [-1/4, 1/2, 1/2, 1/2, -1/4]. \quad (10)$$

From (10), the filters used in Fig. 4 are derived.

Next, the red pixel image R is reconstructed. Assume that the difference image $R - G$ is band-limited to a rate well below the Nyquist rate. The difference image $R - G$ is reconstructed from sampled-difference image $R_1 - G_1$ using

$$R - G = LP * (R_1 - G_1) \quad (11)$$

where LP is a low-pass filter. Using G from (8) solve (11) for R (same technique used to reconstruct B).

3.3. Interpolation Artifact Reduction

Interpolation artifacts are reduced using techniques similar to the iterative algorithms proposed by [3][7][9]. Assume $R - G$ and $B - G$ are slowly varying. Let $median(\cdot)$ denote a median filter operator. The following iterative procedure, performed m times, suppresses small variations in color while preserving edges:

```

repeat_m_times
1.  $R = median(R - G) + G$ .
2.  $B = median(B - G) + G$ .
3.  $G = 1/2 (median(G - R) + median(G - B) + R + B)$ .
end_repeat

```

3.4. Complete Algorithm

The homogeneity-directed demosaicing algorithm is as follows:

1. Reconstruct f_H and f_V , the color images from horizontal and vertical interpolation, respectively. See (8) and (11).
2. Evaluate H_{f_H} and H_{f_V} using (4).
3. Define f

$$f(n) = \begin{cases} f_H(n) & \text{if } A * H_{f_H} > A * H_{f_V} \\ f_V(n) & \text{else} \end{cases} \quad (12)$$
4. Apply the interpolation artifact reduction technique (see 3.3) to f .

3.5. Adaptive Parameterization

The homogeneity maps in step 2 above need parameters δ , ϵ_L , ϵ_C . In this paper, δ is fixed and ϵ_L and ϵ_C are extracted from the scene adaptively. Assume for a moment that the orientation of the object boundary at $n \in X$ is horizontal. In this case, the pixels located immediately to the right and to the left of n are likely to belong to $U_f(n, \delta, \cdot)$. Let $n = [n_1, n_2]^T$, where n_1 and n_2 are horizontal and vertical coordinates, respectively. A good candidate for parameter value ϵ_L at n is,

$$\varepsilon_L = \max\{d_L(f_H(n), f_H(n - [1,0]^T)), d_L(f_H(n), f_H(n + [1,0]^T))\} \quad (13)$$

Likewise, if the orientation of the object boundary at n is vertical instead, then consider

$$\varepsilon_L = \max\{d_L(f_V(n), f_V(n - [0,1]^T)), d_L(f_V(n), f_V(n + [0,1]^T))\} \quad (14)$$

The minimum of (13) and (14) is assigned to ε_L (ε_C done similarly).

4. IMPLEMENTATION AND RESULTS

Bilinear interpolator is used for LP (11). The interpolation artifact reduction step (see 3.3) is iterated 3 times—this is determined empirically. In Fig. 5, the top row shows the test input images, which was sampled using Bayer pattern CFA. The output images from the proposed algorithm appear in the bottom row. Our algorithm is compared to a method developed by Gunturk *et al* [9], shown in the middle row. We encourage reviewing [9], because it has very good comparisons to other demosaicing algorithms. In most cases, the proposed algorithm reduces the level of color artifacts and zippering when compared to [9].

5. CONCLUSION

In this paper, an adaptive homogeneity-directed demosaicing algorithm was presented. Metric neighborhood modeling techniques were used to compare the level of color artifacts that are present in images, and to select the direction for interpolation. Filterbank interpolation techniques were developed to cancel aliasing, and interpolation artifact reduction iterations suppressed color artifacts. Experimental data shows how well the algorithm performs.

6. ACKNOWLEDGEMENTS

The authors would like to thank Agilent Technologies for helpful discussions and encouragement. We also thank B.K. Gunturk for providing the code to his algorithm.

7. REFERENCES

- [1] B. E. Bayer, "Color imaging array," US Patent 3 971 065, 1976.
- [2] D. R. Cok, "Reconstruction of CCD images using template matching," *Prof. IS&T Ann. Conf./ICPS*, 1994, pp. 380-385.
- [3] R. Kimmel, "Demosaicing: Image reconstruction from CCD samples," *IEEE Trans. Image Process.*, vol. 8, pp. 1221-1228, 1999.

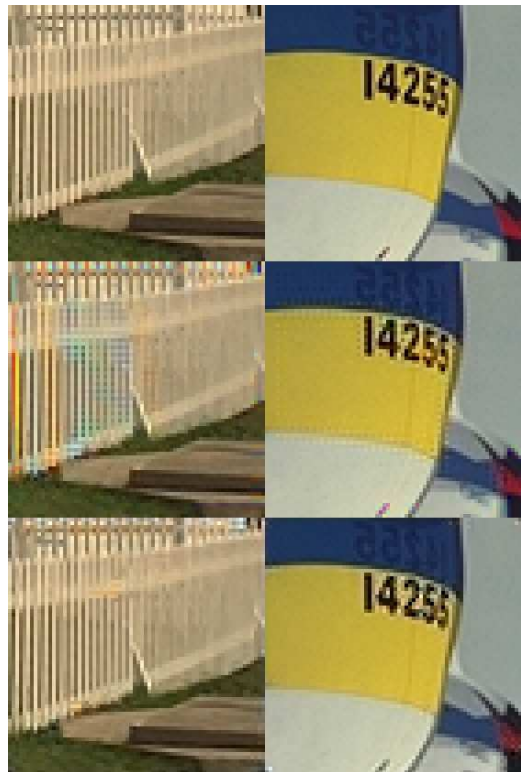


Fig. 5. (top row) original images, (middle row) output from [9], (bottom row) output from proposed algorithm.

- [4] W. T. Freeman and Polaroid Corporation, "Method and apparatus for reconstructing missing color samples," US Patent 4 774 565, 1998.
- [5] J. W. Glotzbach, R. W. Schafer, and K. Illgner, "A method of color filter array interpolation with alias cancellation properties," *IEEE Prof. Int. Conf. Image Process.*, vol. 1, 2001, pp. 141-144.
- [6] J. E. Adams, Jr., "Design of color filter array interpolation algorithms for digital cameras, Part 2," *IEEE Prof. Int. Conf. Image Processing*, vol. 1, 1998, pp. 488-492.
- [7] D. D. Muresan and T. W. Parks, "Optimal Recovery Demosaicing," IASTED Signal and Image Processing, Hawaii, 2002.
- [8] C. A. Laroche and M. A. Prescott, "Apparatus and method for adaptively interpolating a full color image utilizing chrominance gradients," US Patent 5 373 322, 1994.
- [9] B. K. Gunturk, Y. Altunbasak, R. Mersereau, "Color plane interpolation using alternating projections," *IEEE Trans. on Image Process.*, vol. 11, no. 9, 2002.
- [10] CIE, *Colorimetry*, CIE Pub. no. 15.2, Centr. Bureau CIE, Vienna, Austria.
- [11] G. Sharma and H.J. Trussell, "Digital Color Imaging," *IEEE Trans. Image Processing*, vol. 6, no. 7, pp. 901-932, July 1997.
- [12] G. Wyszecki and W.S. Stiles, *Color Science: Concepts and Methods, Quantitative Data and Formulae*, John Wiley and Sons: New York, 1982.
- [13] W. Sweldens, "The Lifting Scheme: A new philosophy in biorthogonal wavelet constructions," *Proc. SPIE 2569*, pp. 68-79, 1995.